THE SHAPE AND AERODYNAMICS OF LARGE RAINDROPS

By James E. McDonald

Iowa State College[1,2]

(Original manuscript received 15 August 1953; revised manuscript received 5 April 1954)

ABSTRACT

The physical factors which might be expected to control the shape of large raindrops are surface tension, hydrostatic pressures, external aerodynamic pressure, electrostatic charge, and internal circulation. Each of these is examined quantitatively, and it is concluded that under most conditions only the first three play important roles in producing the deformation characteristic of large raindrops. By analysis of high-speed photographs of water drops falling at terminal velocity, the distribution of aerodynamic pressures is deduced and is shown to imply that separation in the airflow about a raindrop has very significant effects on drop shape. The surface integral of the vertical components of the deduced aerodynamic pressures is found to be in reasonable agreement with the drop weight. The effect of boundary-layer separation on a number of physical processes occurring at the surface of falling drops is noted briefly.

1. Introduction

It has been known for over half a century that large raindrops do not possess the streamlined form popularly described as the "teardrop" shape. High-speed photographs (Flower, 1928; Edgerton, 1939; Blanchard, 1950) reveal, instead, that a drop falling through the air exhibits a marked flattening on its lower surface and smoothly rounded curvature, rather than conical taper, on its upper surfaces (see fig. 1). This long-recognized peculiarity of large drops has never been adequately explained, and only very few attempts to elucidate this matter have ever been undertaken.

Although Thomson, in 1885, made some observations on the shape of liquid drops moving through various fluids, the first serious attempt to examine the meteorological problem of the shape of large raindrops appears to have been made by Lenard (1904). Using a vertical airstream with water drops suspended freely therein, Lenard carried out a number of experiments on terminal velocities, deformation, and breakup. He noted that a finite time, somewhat greater than a tenth of a second, was required for a large drop to attain its equilibrium degree of deformation. He suggested that this might be due to centrifugal distortion set up by internal circulations, which, for inertial reasons, took a measurable amount of time to become established by the surface friction of the air rushing past the drop. To the present writer's knowledge, no extension of this interesting beginning of the study of the drop-shape problem was made for more than forty years following Lenard's work. Flower (1928), in a study of falling speeds, had found it necessary to appeal to Lenard's theory of centrifugal distortion; and even when Laws (1941) carried out his very extensive measurements of the terminal velocity of water drops, no other theory of drop deformation was available to be invoked to account for the marked distortion of large drops, and this despite the fact that the reality of Lenard's postulated circulations had never been demonstrated.

Spilhaus (1948), in a short paper on raindrop shape and falling speed, has made the only other contribution to this problem that has come to the writer's attention. Spilhaus suggested that the vertical flattening of large drops is due to the combined action of surface tension and aerodynamic pressures. This was the first introduction into the raindrop problem of any consideration of the role of the aerodynamic factor, although Kluesener (1933) had made very similar suggestions about the flattening of fuel-spray droplets. Spilhaus pointed out that, due to the deficit of external pressure around the waist of a drop, "the drop must deform so as to reduce the ratio of its area of cross section to perimeter in the vertical plane" in order to give the surface tension an opportunity to equilibrate the aerodynamic forces. Spilhaus may not have been aware of Lenard's earlier work, for he neither mentions it specifically nor gives any consideration to the centrifugal effects which Lenard held to be solely responsible for producing drop deformation. Neither Spilhaus nor Lenard offered any explanation of why large drops are not symmetrical about horizontal planes through their centers, and Spilhaus explicitly omitted this asymmetry from his theory in order to be able to use experimental data on drag coefficients of oblate ellipsoids. As will be pointed out below,

[1] The research reported here was initially supported by the Office of Naval Research, under Contract Nonr-757(00), Project NR 082 093. It was completed at the University of Chicago, with sponsorship of the Geophysics Research Directorate, Air Force Cambridge Research Center, under Contract AF 19(604)-618.

[2] Present affiliation: University of Arizona.

Spilhaus used an incorrect relationship for determining the surface-pressure increment due to surface tension, and also overlooked the significant effects of internal hydrostatic pressure gradients present in a drop falling at terminal velocity. With this background to the present problem, it seems appropriate to conclude that the issues involved are far from settled. In the present article, some further contributions to this problem will be made, and the results used to gain an improved understanding of some important features of the airflow about large raindrops.

2. Factors controlling raindrop shape

In the course of the present study, an effort has been made not only to gain a better appreciation of the role of centrifugal distortion, surface tension, and aerodynamic pressures, but also to obtain a clearer recognition of the possible importance of electrostatic charges and internal hydrostatic pressure gradients.

The *only* reason that water drops can exist at all as mechanically stable systems is that surface forces at the water-air interface continually try to minimize the interfacial area. When this effect of surface tension acts alone, or nearly so, as in the case of cloud drops, drizzle, and even small raindrops, it succeeds in molding a drop into the shape characterized by minimum surface-to-volume ratio, *i.e.*, a sphere. When, however, other factors than surface energy contribute significantly to the total energy of the drop, minimum total energy may become inconsistent with perfectly spherical shape. One might hope to assemble all of these other energy factors, express mathematically their contributions to the total drop energy, and then determine the equilibrium shape by minimizing the total energy with respect to some suitable shape parameter or parameters. If the gravitational effects (hydrostatic pressures) were the only additional energy factor, this might be done here just as it has been done (by tedious numerical processes) for the case of pendent and sessile drops (Adam, 1949). However, the very great difficulty of incorporating the *aerodynamic* factor into this type of approach precludes any analysis which treats it as a classical minimal problem. Recognizing this, the writer has sought to approach the problem simultaneously from two directions in order to converge ultimately upon a result (deduced aerodynamic pressure distribution) whose correctness may be judged tolerably well by comparison with certain experimental results in the fields of fluid dynamics and cloud physics, as well as by a quantitative comparison of pressure drag and drop weight. The central idea in this analysis has been to evaluate all the factors controlling the pressure distribution *inside* a large drop and then, with the use of certain surface physical concepts, to determine the surface pressure prevailing in the boundary layer just outside the drop surface. If the surface-pressure pattern thus deduced is found to be in reasonably good agreement with aerodynamic principles (as will be shown to be the case), some confidence may be placed in the theory of drop shape on which the calculations have been based. The logic of this approach will be further elaborated below.

Surface tension.—As a consequence of the net inward attraction exerted on the surface molecules by the molecules lying deeper within the drop, the surface tension of the water in a raindrop produces an

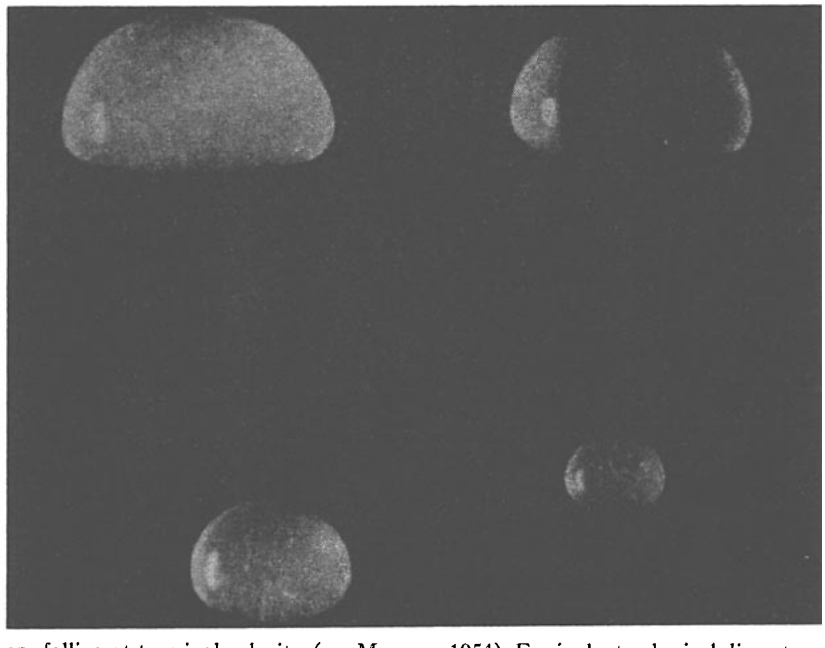

FIG. 1. Large water drops falling at terminal velocity (see Magono, 1954). Equivalent spherical diameters and measured fall velocities as follows: upper left, 6.5 mm and 8.9 m/sec; upper right, 6.0 mm and 8.8 m/sec; lower left, 4.8 mm and 8.3 m/sec; lower right, 2.8 mm and 6.8 m/sec.

increase of pressure within the drop over and above that prevailing in the air outside. This increment in pressure, Δp_s, at a given point on the drop surface, is given, in general, by

$$\Delta p_s = \gamma(1/R_1 + 1/R_2), \qquad (1)$$

where γ is the surface tension of the water-air interface, and R_1 and R_2 are the principal radii of surface curvature at the point in question (Adam, 1949). The quantity Δp_s can be either positive or negative, if one admits sufficiently arbitrary surface geometry. A principal radius will here be regarded as positive for the case where the water-air interface is convex as viewed from the air, and Δp_s then becomes the water pressure just inside the drop minus the (aerodynamically controlled) air pressure just outside the interface at the point in question.

In the special case of a spherical drop, $R_1 = R_2 = r$, where r is the drop radius, and then

$$\Delta p_s = 2\gamma/r. \qquad (2)$$

This restricted equation (2) was inappropriately applied by Spilhaus to his assumed ellipsoidal raindrops: he used for r the radius of the circular cross-section in a horizontal symmetry plane. Since this radius is only one of the two principal radii of curvature at a point on the waist of such a drop, and since the second principal radius is there smaller than the first, Spilhaus underestimated the pressure increment, particularly for his large, and hence very much flattened, drops. At the same time, he neglected to consider the fact that the surface pressure increment is different, in general, at each different point of the drop surface, a matter of fundamental importance in the drop-shape problem, as will be shown below.

A technique for determining R_1 and R_2 from a photograph of a falling drop will be explained below.

Internal hydrostatic pressure.—In a coordinate system moving with a drop which is falling at its terminal velocity, an observer would regard the drop as being just supported against gravity by the vertical components of the aerodynamic pressure forces and the surface shear stresses due to the apparently upward-rushing air. Consequently, there must exist within the drop a vertical pressure gradient of exactly the sort found in any mass of fluid at rest in a gravitational field. This hydrostatic pressure gradient appears to have been overlooked by both Lenard and Spilhaus; yet, in the limit of very large raindrops, the difference in hydrostatic pressure between top and bottom of a drop becomes quite important in controlling drop shape.

TABLE 1. Values of surface-pressure increment due to surface tension, top-to-bottom hydrostatic pressure difference, and stagnation pressures for *spherical* drops of various radii, and density ρ_w, at 0C, falling at terminal velocity V_t through air of density ρ.

Radius, r (cm)	$\Delta p_s = 2\gamma/r$ (dyne/cm²)	$2\rho_w gr$ (dyne/cm²)	$\frac{1}{2}\rho V_t^2$ (dyne/cm²)
0.001	150,000	2.0	0.001
0.01	15,000	19.6	3.4
0.05	3,000	98.0	105
0.10	1,500	196	273
0.20	750	392	506
0.30	500	588	550
0.40	375	784	*
0.50	300	980	*

* Data on V_t, taken from Gunn and Kinzer (1949), do not include drops of $r > 0.3$ cm.

Table 1 illustrates the comparative values of the surface-pressure increment, Δp_s, the top-to-bottom hydrostatic pressure difference, $2\rho_w gr$, and the stagnation pressure, $\frac{1}{2}\rho V_t^2$, for a number of different drop sizes, extending from those in the cloud-particle range up to the largest stable water drops. Note carefully that in computing the values of Δp_s and $2\rho_w gr$ given in the table, the drops are assumed to be *spherical*, so the numerical magnitudes must not be regarded as exact for drops much larger than about 0.05 cm in diameter.

It may be seen from table 1 that hydrostatic effects are negligible compared to surface tension effects for water drops of radius less than about 0.05 cm, but that the hydrostatic pressure differential is equal to or greater than the surface-pressure increment for large raindrops. Table 1 also shows that, for drops of cloud-particle size, the surface-pressure increment is so very large compared with hydrostatic pressure differences within the drop, or compared with the minute aerodynamic pressures established at terminal velocity, that each of these factors (and also all others) may safely be neglected in discussing drop shape. Hence *cloud* drops do simply assume the shape implying minimum surface free-energy, thus accounting for their well-known spherical form. But in the case of a raindrop at the upper end of the observed drop-size distribution, the surface-pressure increments are only of the same order of magnitude as the pressure effects due to gravity and aerodynamic factors, so for this case one must examine the shape problem more thoroughly.

Electrostatic charges.—Since it is known that hydrometeors of all sizes, ranging from cloud droplets up to the largest raindrops, may acquire electric charge, it is necessary to consider the possibility that the drop-shape problem might be sensibly affected by this factor.

By *electrostatic* standards, the water in a natural raindrop is a good conductor. It can be shown (*e.g.*, Jeans, 1941) that a conductor carrying a local surface charge-density σ experiences an *outward*-directed tension (negative pressure) whose magnitude per unit area is given by

$$T = 2\pi\sigma^2. \qquad (3)$$

This electrostatic tension opposes the surface tension,

and thus constitutes one of the several destabilizing factors that control drop morphology. This point assumes real interest as soon as one notes that, on any conductor of variable surface curvature, there is a tendency (counteracted only by external fields due to neighboring charged bodies) for the charge to distribute itself in such a manner that σ becomes largest where the surface curvature is largest. Hence, as a charged raindrop begins to flatten out due to aerodynamic effects, more of the total available charge should migrate towards the waist of the drop, and should there produce a locally exaggerated suppression of the surface tension effect, which serves to oppose the effect of low aerodynamic pressures near the waist. The drop should relax into a state of still greater deformation, and this further flattening should then not only further decrease the external air pressure at the waist, due to continuity and Bernoulli effects in the airflow, but should at the same time have the additional unfavorable effect of calling for still further buildup of surface charge-density near the increasingly sharply curving waist. This should, in turn, oppose even more strongly the surface tension effects that are serving to hold the drop together, and so on, until the drop becomes so flattened as to be torn apart by aerodynamic forces. This qualitative picture suggests a plausible mechanism for the breakup of large raindrops in thunderstorm precipitation-currents, but it will next be shown that this interesting hypothesis is quantitatively tenable only for quite abnormal degrees of charging of the drops.

In the region just outside a point on the surface of a raindrop having local surface charge-density σ, the electric field intensity is

$$E = 4\pi\sigma. \tag{4}$$

Now, the greatest possible value that σ can assume is given by (4) when E is set equal to E_d, the dielectric strength of the surrounding air. Any greater surface charge will induce corona discharge that will reduce E to E_d. E_d is pressure dependent and is also sensitive to the geometry of the charged conductors involved, but, for the cloud-physics problem at hand, it will be conservative (in the sense of admitting rather high values of σ and hence of T) to put $E_d = 30{,}000$ volt/cm in (4), solve for the implied surface charge-density, and then insert this into (3) to determine the greatest value T can assume before corona discharge sets in. The result is:

$$T_d = \frac{2\pi E_d^2}{(4\pi)^2} = \frac{E_d^2}{8\pi} = \frac{10^4}{8\pi} = 400 \text{ dyne/cm}^2,$$

for the sea-level value of $E_d = 30{,}000$ volt/cm $= 100$ e.s.u. At the 500-mb level, where E_d falls to about 15,000 volt/cm, T_d could be no greater than 100 dyne/cm^2. At 700 mb, the limit is about 200 dyne/cm^2. It is to be noted that T_d is independent of drop size; hence, the condition favoring large relative importance of electrostatic effects as compared to surface-tension effects will be large drop radius.

This electrostatic effect (decrement of pressure on passing from the air side over into the water side of the drop surface) is of the order of magnitude of Δp_s for rather large drops as calculated above, but T_d has been computed here for a value of σ that is substantially larger than any yet observed directly or indirectly. Gunn (1947; 1950) has found, by direct measurement from aircraft flying through precipitating clouds, that drops seldom bear charges in excess of 0.1 e.s.u. Furthermore, his values were notable in that they are almost an order of magnitude greater than those previously reported for raindrop charge as measured at the earth's surface (Chalmers, 1949). Gunn (1949) has given an interesting possible explanation of why raindrops may not be able to accumulate charge to such a degree as to produce corona discharge of the type here tacitly assumed (isolated drops discharging into the air), so that his observation is not without theoretical support.

Now, a drop of radius r carrying so high a charge density as to imply $E = E_d$ at its surface, bears a total charge $q_d = r^2 E_d$. At 700 mb, roughly the pressure level at which Gunn found the highest particle charges, $E_d \approx 70$ e.s.u. Hence, for an excessively large drop of the sort which might conceivably result from the melting of a hail particle, say $r = 0.5$ cm, $q_d = 17.5$ e.s.u., or two orders of magnitude greater than Gunn's observed maximum charge of about 0.1 e.s.u. For a precipitation particle of more plausible size, say $r = 0.05$ cm, $q_d = 0.17$ e.s.u., which is in rough agreement with Gunn's maximum observed value. However, for any and all drops charged to the dielectric limit near 700 mb, $T_d \approx 200$ dyne/cm^2, and when one considers drops of radii as small as 0.05 cm, Δp_s is already appreciably greater than 200 dyne/cm^2. Table 1 shows $\Delta p_s = 1500$ dyne/cm^2 for the spherical approximation at this drop size. For drops of radii near 0.35 cm, T_d becomes about equal to Δp_s, so if cloud electrical processes are capable of charging such large drops to the limit q_d, electrostatic deformation will be important.

It would seem, however, that attractive as the electrostatic factor seems in explaining drop shape and breakup, such observations of drop charges as do exist indicate its slight quantitative importance under most circumstances. The electrostatic factor must be held in mind as possessing possible significance in processes occurring in the regions of highest electrical activity of thunderstorms, particularly if future studies reveal that drop sizes are excessive in just such regions, but elsewhere it may be ignored on the basis of existing drop-electricity measurements. It may be noted that

in the regions of peak field strength within thunderclouds, the shape problem must also be considered in relation to the Macky effect due to external electric fields (Macky, 1931), but this case will not be treated in the present article.

Finally, it is to be noted that the electrostatic factor is definitely not to be considered in the shape analysis carried out below, for that analysis concerns uncharged water drops formed under laboratory conditions.

Internal circulations.—When the boundary of any airflow is a solid, as in the case of flow over an airfoil, the "condition of no slip" for real fluids implies that the air in contact with the boundary is at rest relative to that boundary. But when the boundary is the surface of a liquid, as in the case of a raindrop falling through the air, the no-slip condition can be satisfied even if the surface layer of air is slowly moving, for the interfacial liquid may be drifting downstream at some slow rate. In the case of a falling raindrop, any such surface circulation induced by shear stresses exerted by the ambient air would in turn induce some sort of axisymmetric internal circulation.

Lenard (1904) *postulated* the existence of such internal motions, and regarded them as capable of accounting for the drop deformations which he had observed; but he made no attempt to demonstrate their reality experimentally, nor to predict their intensity theoretically. Qualitatively, one can say that at least a very slow internal circulation is almost inevitable, for the dynamic boundary condition pertinent here is that of continuity of tangential shear stress across the water-air interface; and since water's viscosity is not infinite, at least a slight amount of internal motion seems certain to develop. In the analysis that will be given below, it will be necessary to know whether the pressure at a point on the vertical axis of a drop is equal to that at a point at the same height above the base of the drop but lying just inside the drop surface. In view of the relatively small radii of curvature of the water-particle trajectories in any internal circulations, one can show that horizontal uniformity of pressure would be noticeably altered if surface water-velocities of much over one-tenth the drop's falling speed can be developed. Consequently, it becomes indispensable here to obtain some estimate of the intensity of the internal circulation.

Bond (1927) has examined theoretically the problem of internal circulations for the case of a liquid sphere moving through a dissimilar liquid medium for the case of Reynolds numbers in the Stokes-law range, and has shown that the development of internal circulations does not depend on simply the external Reynolds numbers, but rather on the *relative viscosity* of the interior and the exterior fluids.

Richardson (1950) has made some experimental studies of the breakup of water drops falling from a tower 125 ft high, and has suggested that their breakup is due to the effects of internal circulation; but he appears to have obtained no direct evidence to support this view. He did observe that drops of a very viscous liquid (thickened methyl salicylate) resisted breakup far more effectively than did water drops, and argued that this was due to their resistance to the development of internal circulations. One can question this interpretation on the ground that the increased viscosity may also play an important role in suppressing breakup by inhibiting the rapid internal motions that probably accompany breakup in oversize drops (Blanchard, 1950).

Blanchard (1949) attempted to observe internal circulations in water drops suspended in a vertical wind tunnel. He introduced fine particles of alumina into the drops to serve as tracers in revealing internal motions, but reported no evidence for any circulations. His observations may be inconclusive, due to the fact that his tracer particles might have been too large ("300 microns and under") to be carried along in currents of the order of centimeters per second. Kinzer (unpublished) has observed very slow, rolling motions inside drops containing fine talc particles, but he estimated the velocities involved to be less than a centimeter per second, which can be shown to be too slow to have appreciable centrifugal effect on drop shape.

Because of the importance of settling the question of whether internal circulations should be important in the drop-shape problem, the writer has sought a theoretical basis for estimating the upper limit to the circulation velocities that could develop within a large drop falling at the experimentally established limiting speed of about 8 m/sec. The analysis is based upon the following assumptions:

1. The shear stress is continuous across the water-air interface;
2. The condition of no slip holds, but the interfacial molecules of water and air drift together so slowly downstream that, as far as the external flow dynamics are concerned, the surface air-molecules' speed may be assumed to be negligibly small compared to the relative airspeed at the outer limit of the laminar layer (about 12 m/sec at the waist of a large drop falling at 8 m/sec);
3. The drop remains spherical; a corollary to this assumption is the implication that the stream function inside the drop corresponds to that of a spherical vortex.

Any exception to assumption (1) would imply finite shear stress acting on an infinitesimal lamina of fluid, *i.e.*, infinite accelerations would result from any failure for this condition to hold, so this first assumption is above reproach. That the surface air-velocity at the base of the boundary layer may be regarded as zero compared to that prevailing just outside the boundary layer [assumption (2)] is an assumption that can only be tested *a posteriori*. It will be shown below to be admissible. Assumption (3) is introduced to simplify the analysis, even though it fails to hold in the case of interest here. However, departure from sphericity

ought not have any large effect on the chances for the development of internal circulation, since the experimental work of Garner (1950) and Spells (1952) demonstrates that the type of vortices predicted by Bond (1927) appears in large drops of liquid in liquid despite a very marked deformation. Assumption (3) simplifies the analysis primarily because of the corollary implication concerning the nature of the internal stream function. For a spherical drop, the stream function for a spherical vortex may be used to describe the motion to within an approximation that is adequate for the present purposes.

The general form of the stream function ψ for an axisymmetric flow, when specialized to the case of motion within a sphere, reduces to the form

$$\Psi = A(r^2 - a^2)r^2 \sin^2\theta, \tag{5}$$

where A is a constant, a the radius of the sphere, r the radial coordinate measured from the center of the sphere, and θ is the meridional coordinate measured from a polar axis directed towards the pole of the sphere towards which fluid moves along the polar axis (see fig. 2 and Milne-Thomson, 1949).

The meridional water velocity u', at a general point (r, θ), is given by

$$u'(r, \theta) = \frac{1}{r}\left(\frac{\partial\psi}{\partial r}\right)_{r,\theta} = A(4r^2 - 2a^2)\sin^2\theta. \tag{6}$$

Hence,

$$u'(a, \tfrac{1}{2}\pi) = 2a^2A. \tag{7}$$

Also, the velocity shear just inside the surface of the sphere at its waist is, from (6),

$$(\partial u'/\partial r)_{a,\frac{1}{2}\pi} = 8aA. \tag{8}$$

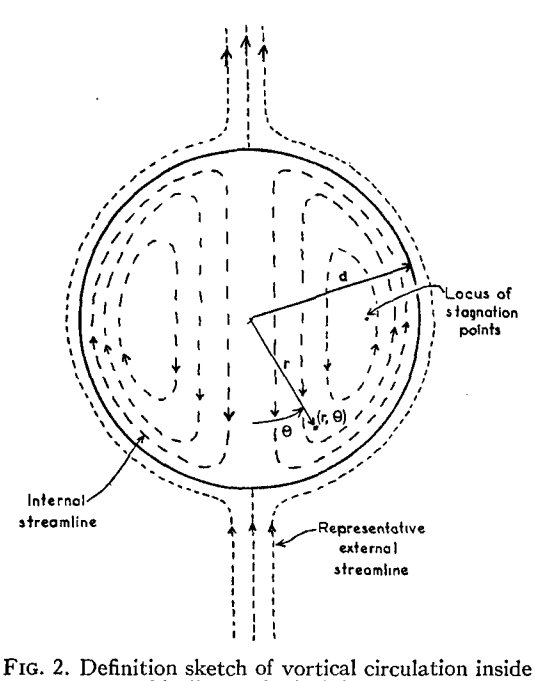

FIG. 2. Definition sketch of vortical circulation inside idealized spherical drop.

So, from combination of (7) and (8) to eliminate A, it follows that

$$u'(a, \tfrac{1}{2}\pi) = \tfrac{1}{4}a(\partial u'/\partial r)_{a,\frac{1}{2}\pi}, \tag{9}$$

and the problem of determining $u'(a, \frac{1}{2}\pi)$ becomes that of finding $\partial u'/\partial r$ at the same point. This can be done next with the aid of assumption (1).

Continuity of shear stress across the water-air interface requires

$$\mu'(\partial u'/\partial r)_a = \mu(\partial u/\partial r)_a,$$

where the primed quantities refer, as before, to the water, and the unprimed to air. Since $\mu' \approx 10^2\,\mu$, one has

$$(\partial u'/\partial r)_a \approx 10^{-2}(\partial u/\partial r)_a. \tag{10}$$

The velocity shear in the boundary layer of air just outside the drop is of the order of u_1/δ, where u_1 is the local air speed relative to the sphere at the outer limit of the laminar boundary layer, and δ is that layer's radial thickness. Since outside the boundary layer the flow at raindrop Reynolds numbers will be essentially potential flow, at least up to about the waist of the drop, and furthermore since to assume potential flow is to be conservative here in the sense of admitting rather large waist velocities in the air flow, u_1 is taken as 1.5 U_0, where U_0 in the raindrop case is the terminal falling velocity. On the other hand, to evaluate δ, the boundary-layer theory of Tomotika (1935) will be utilized. Tomotika showed that, for a point about 80 deg from the forward stagnation point of a sphere,

$$\delta \approx (6.8/u_1)(2U_0\nu a)^{\frac{1}{2}}, \tag{11}$$

where ν is the kinematic viscosity of the air, and a is the radius of the sphere. For $U_0 = 8$ m/sec and $a = 0.5$ cm, δ is found from (11) to be about 0.05 cm. Hence, near the waist of such a large drop, $(\partial u/\partial r)_a \approx u_1/\delta = (1200)/(0.05)$ sec^{-1} $= 2.4 \times 10^4$ sec^{-1}, and then from (10), $(\partial u'/\partial r)_a \approx 240$ sec^{-1}.

Combining this last result with (9), one finds that $u'(a, \frac{1}{2}\pi) \approx 30$ cm/sec. It is to be noted immediately that, since this speed is less than 3 per cent of the air speed (12 m/sec) at the outer limit of the boundary layer near the waist of a drop falling at the maximum speed of about 8 m/sec, assumption (2) is rendered quite plausible *a posteriori*. If a similar calculation is carried out for the more probable value of 2.5 mm for the radius of a "large" drop, the circulation velocity at the waist is found to be only about 20 cm/sec, which is in still closer accord with assumption (2).

The circulation intensities so predicted are substantially higher than those observed by Kinzer (in smaller drops), and it will become possible below to point out a very good reason why the actual circulations fail to reach the intensity just predicted. However, since this point will depend upon a deduction which hinges

in part upon the negligibility of internal circulations, it is here necessary to proceed to show that even a surface motion of 30 cm/sec in a large drop will not lead to internal pressure gradients large enough to alter seriously the hydrostatic balance inside the drop. Consider the radially inward force that would develop as a centrifugal reaction to the here predicted vortical motion. The radii of curvature of the trajectories of particles moving just inside the boundary of a spherical vortex near its waist are nearly identical with the radius, a, of the vortex boundary, as may be seen in fig. 2. Since the speed of circulation falls off rapidly inward ($u' \propto r^2$) as one approaches the ring of stagnation points lying in an equatorial circle at $0.71\,a$ from the axis, and since furthermore the centrifugal reaction varies as the square of the circulation velocity, one will obtain a reasonable order-of-magnitude estimate of the centripetal force involved if he assumes that a lamina of radial thickness equal to about one-tenth the distance from the surface to the stagnation point moves meridionally near the waist with the predicted speed of 30 cm/sec in a very large drop of 0.5-cm radius. The centripetal force per unit area acting on this lamina is found to be about 30 dyne/cm^2. This contribution to the internal pressure field is only 10 per cent of the surface-tension contribution of about 300 dyne/cm^2 for a drop of this size, and is still a smaller fraction of the hydrostatic pressure difference from top to bottom of such a drop. For a drop of 0.25-cm radius (still a very large raindrop), one finds that the centrifugal pressure effect represents a still smaller fraction of the surface-tension incremental pressure. Although the preceding analysis can only be regarded as a relatively crude approximation, the order of magnitude of the predicted centrifugal pressure gradient appears to warrant neglect of internal circulation within falling raindrops, at least as far as such circulations might affect the shape of drops in the range of sizes now known to occur in natural rain. This conclusion will be considerably strengthened below, when the phenomenon of separation is discussed.

Aerodynamic pressure distribution.—In the writer's opinion, all the factors capable of influencing drop shape, with the important exception of the aerodynamic factor, have now been considered. The next logical step for completing the drop-shape theory should thus be a direct evaluation of these aerodynamic pressure effects. Unfortunately, to carry out this last step would be extremely difficult. Without belaboring this fairly obvious point, we may note that the aerodynamic pressure distribution over the surface of a drop falling through the air is itself determined by the very shape one wishes to deduce. One could only proceed here, in principle, by some method of successive approximations in which each aerodynamic pressure calculation (based on the previous iterative approximation to the equilibrium shape) would be used to deduce a modified shape consistent with the surface-tension and hydrostatic-pressure requirements, and then this new shape would have to be used in the next iteration of the aerodynamic calculations, and so on. Difficult as this would be, one might be ready to attempt it, were it not for the fact that there exists no general method for calculating analytically the pressure pattern about an arbitrary surface. The method of superposition of a suitable array of sources and sinks, which is sometimes useful in treating the flow around revolutes, is only sufficiently convergent to be practicable in the limit of very elongated revolutes. To proceed with an iterative method in which each aerodynamic calculation had to be performed graphically or numerically was one course open to the writer; but he has instead chosen to proceed at this point by a different approach: namely, to analyze photographs of actual drops of known size and falling speed in order to *deduce* these aerodynamic pressures which would be so difficult to calculate directly.

3. Calculation of aerodynamic surface pressures

On the basis of the discussions of drop shape given in the preceding section, the writer adopts the following hypothesis: *The equilibrium shape of a large drop, bearing at most a charge small compared to the limiting value imposed by the dielectric strength of air and falling at terminal velocity, is that particular shape for which the joint action of the external aerodynamic pressures and the surface-pressure increments just produces an internal pressure distribution that satisfies the hydrostatic equation within the drop.*

This hypothesis has led the writer to employ the following method for calculating the aerodynamically developed external surface pressures. Given a photograph of a drop of known size and falling speed, one first calculates the stagnation pressure developed at the *lower* pole of the drop. It is fortunately one of the well established facts of fluid dynamics that, regardless of almost all peculiarities of a given flow pattern about an object immersed in a fluid stream, the excess pressure developed at the leading stagnation point is $\frac{1}{2}\rho v^2$, where ρ is the fluid density and v is the speed of the fluid far from the object, measured relative to that object. Hence, this first step involves no approximations. Next one measures, on the available photograph, the radius of curvature R_0 of the drop-surface profile at the lower stagnation point. For reasons of axial symmetry, $R_1 = R_2 = R_0$ at this point of the drop, *i.e.*, the drop surface is locally a portion of a sphere of radius R_0 at the stagnation point. Using this measured radius in (1) to compute Δp_s at the stagnation point, and *adding* the result to the computed stagnation pressure, one obtains the pressure prevailing just *inside* the drop at its lower pole. Next, using the hydrostatic

equation, one may quickly determine the internal pressure $p_i(z)$ at any height z, measured upward along the vertical axis of symmetry from zero at the lower pole. Then, as long as internal circulations produce only negligible internal pressure gradients, the pressure *just inside* the drop surface at height z is equal to that already determined for the point along the axis at that height. Finally, if one can determine from the drop photograph the values $R_1(z)$ and $R_2(z)$, (1) can be used to compute $\Delta p_s(z)$. *Subtraction* of this from $p_i(z)$ yields $p_e(z)$, the external aerodynamically induced pressure at height z.[3]

From the preceding discussion it can be seen that the success of this method hinges upon being able to determine $R_1(z)$ and $R_2(z)$ from a single side-view photograph of a given drop. The technique for doing this turns out to be quite straightforward.[4]

One of the two principal radii of a revolute, say $R_1(z)$, turns out to be simply the radius of curvature of the meridional profile at the height z. This can be measured on a tracing made from an enlargement of a photograph of the vertical cross-section, such as the one shown here in fig. 1. One constructs normals to the profile curve at each of a fairly dense series of points spaced regularly along the profile, and from these the values of $R_1(z)$ can be determined by measuring the distance along the normal at z to the point of intersection with the normal drawn from the next adjoining point on the profile. In fig. 3, the distance R_1 for point P is shown as PC_1.

$R_2(z)$ is even more easily determined, since this second principal radius, for a surface of revolution, can be shown[4] to be simply the distance from the profile point at z to the axis of revolution measured along the local normal to the profile at z. In fig. 3, R_2 is shown as the distance PC_2. The normals already constructed in the process of finding $R_1(z)$ facilitate rapid determination of $R_2(z)$.

A method for determining $p_e(z)$ having been established, there remains only the question of availability of suitable photographs. The writer has succeeded in obtaining only four photographs from which size and terminal velocity could be accurately determined for water drops that had attained a stable configuration. These photographs, reproduced here in fig. 1, were taken by Magono (1954). All of the remaining discussion is necessarily based upon these four photographs.

Since only the equivalent spherical diameters of the drops in fig. 1 were known, the exact distance scale of each photograph had to be determined preliminarily. On a tracing of an enlargement of each photograph, the cross-sectional area of the drop was divided into a large number of horizontal strips of equal vertical width Δz. Next, for each such narrow strip, the radial distance r_i was measured from a point on the axis of revolution (midway between the upper and lower edges of the strip) out to the meridional profile curve. Then the quantities $\pi r_i^2 \Delta z$ were computed for each of the entire series of strips, and their sum equated to the actual drop volume as given by Magono. From this equality, the scale factor of each enlargement was ascertained for use in converting all subsequently measured lengths to true lengths.

To determine $R_1(z)$ and $R_2(z)$ from drop photographs, it was necessary to find, first, a technique for graphically constructing the normal at an arbitrary point of a smooth curve, and second, a method of faithfully reproducing the drop profile from an enlargement of the original photograph.

After rejection of several methods of constructing normals, a simple optical device was selected as the most precise method for constructing normals. A 45–90 deg crown-glass-prism of 2.1-cm hypotenuse and 1.5-cm length was cemented, hypotenuse-face down, into a rectangular hole just the size of the hypotenuse face, cut in the middle of a 10-cm square sheet of plastic 2 mm thick. A hairline was scribed on the underside of the plexiglass sheet, so as to be colinear with the 90-deg edge of the prism when viewed from directly above. When such a device is placed over any curve for which the normal is sought at some arbitrary point which has been marked with a small dot, one can, by looking down on the 90-deg edge of the prism, see two images of the dot and two images of the curve in the neighborhood of that dot. The geometrical optics of the arrangement can be shown to be such that, if the two images of the curve join with no discontinuity when the two images of the marking dot

[3] Note that all pressures represent algebraic excesses over the prevailing barometric pressure, and that the slight variation in the latter through the height interval spanned by the drop at any instant is ignorable because it is only of the order of 10^{-3} times the internal hydrostatic pressure variation in the same interval.

[4] The writer is indebted to Dr. J. M. Keller of Iowa State College for examining and solving the problem in differential geometry that underlies the technique for determining the principal radii. His solution is too lengthy to be reproduced here, and the writer knows of no published solution. However, subsequent to Dr. Keller's solving this problem, the writer came across a brief statement (Adam, 1949) which agrees with his result and implies that the same problem has been treated previously.

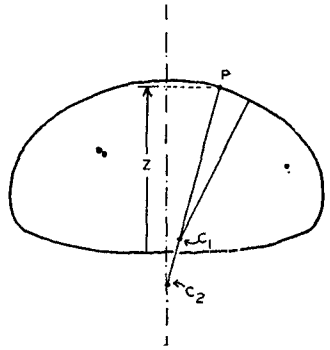

FIG. 3. Definition sketch for method of determining $R_1(z)$ and $R_2(z)$ for any point P on profile of drop. For point P, $R_1(z) = PC_1$, and $R_2(z) = PC_2$.

are equidistant from the 90-deg edge, the latter edge (and hence also the hairline) is normal to the curve to within an error which depends only on the rate of change of curvature near the point of interest.[5] Experience quickly reveals that it is essential to employ a prism having no bevel on the 90-deg edge, and analysis of the optics involved shows that accuracy is improved by using a prism of small hypotenuse. With the particular prism used in the present work, the precision with which normals could be determined was better than the precision of any other step in the analysis. In a total of 110 trial determinations of the normals of circular arcs of several sizes ranging from radii of 2.5 to 15 cm, the absolute errors and the coefficients of variation were all slightly below 1 per cent.

The second graphical problem, that of reproducing the profile, would seem simpler but actually proved to introduce the largest source of error in the entire analysis. The definition of the edges in the highly (roughly 50-fold) enlarged drop photographs was not sharp enough to permit use of the prism device directly on the enlargements. Even the most careful job of freehand copying of the profile produced far too many small irregularities that cancelled the precision attainable with the prism method, so it was decided to fit a series of sections of French curves to the photographic profiles, to obtain at least sectionally smooth curves for analysis. From a large set of such curves, members were selected by a purely trial-and-error procedure until the best fit was secured. It was possible to synthesize all profiles without using more than five separate sections in representing any one profile, still keeping the resultant curve everywhere closer than 1 mm to the photographic profile (order of 1 per cent of the typical radii of curvatures of the enlarged profiles). Although such synthetic reproductions appeared excellent to the eye before analysis began, the results of determinations of the associated normals revealed that there were frequently appreciable discontinuities (order of 10 per cent) in the values of $R_1(z)$ across the junction of two fitted sections. Particular examples of the effects of this type of error will be cited below.

Proceeding in the manner now outlined, the writer determined $p_e(z)$ from the four drop photographs reproduced here in fig. 1. To obtain an estimate of the precision of the method, and to determine how significantly $p_e(z)$ would differ for the two sides of each drop, the two half-profiles (left and right) were treated separately for each drop, and for each half-profile two entirely independent analyses were performed, thus yielding sixteen analyses in all. For any one half-profile, the process of fitting French curves to the photographic profile was done in two wholly independent operations on different days, so that full opportunity for subjective variations in selection of particular curves would obtain. It was found, thereby, that a given half-profile was usually synthesized with different members of the set of French curves in the two cases, that the two resultant curves appeared to the eye to be virtually identical, but finally that the two calculated sets of $p_e(z)$ values exhibited discrepancies which were always most marked at points where one of the two half-profiles had a junction between adjoining fitted sections.

A conventional smoothing formula, $\frac{1}{4}(a + 2b + c)$, was applied to the series of measured values of R_1 and R_2, to suppress somewhat the occasional fluctuations caused by junction errors and chance errors in determinations of normals. It will be seen that such smoothing is in order here, by virtue of the fact that a single normal constructed with a slight error in direction always raises one R_1 value and lowers another. This smoothing did not eliminate junction errors; but from the absence of marked irregularities within portions of the profile curves not influenced by junction effects, it was concluded that it sufficed to remove most of the random errors associated with the use of the prism device.

4. Discussion of results

The results of all sixteen analyses are shown in fig. 4. For each one of the four drops, the mean $p_e(z)$ values obtained from all analyses for that drop are plotted as dashed curves. The scatter about the mean curve, and particularly the difference between the two half-profiles for a given drop, as well as the discrepancies between results of the two analyses performed on any one half-profile, can be deduced by inspection of the plotted points.

In every case, the mean aerodynamic pressure profile exhibits three characteristic features. First, there is a region on the underside of each drop where the pressure rapidly falls from its large positive value at the lower stagnation point to a large negative value at a point lying generally well below the point of maximum cross-section of the drop. Second, there is next a short region of the profile within which the external pressure rises rather sharply to less negative values, steadying off at about the point of maximum cross-section (except for the smallest drop). Third, the remainder of the pressure profile is characterized by generally irregular variations (random-error effects) about moderate negative values, tending in most cases to become more negative near the top of the drop.

Before discussion of the interpretation of these mean profiles, some of the effects of errors on the individual analyses will be noted. The greatest dispersion of computed pressures occurs for the 2.8-mm drop (fig. 4, top

[5] No published description of this device is known to the writer. Mr. K. H. Jehn, of the University of Texas, pointed out the basic principle to the writer several years ago.

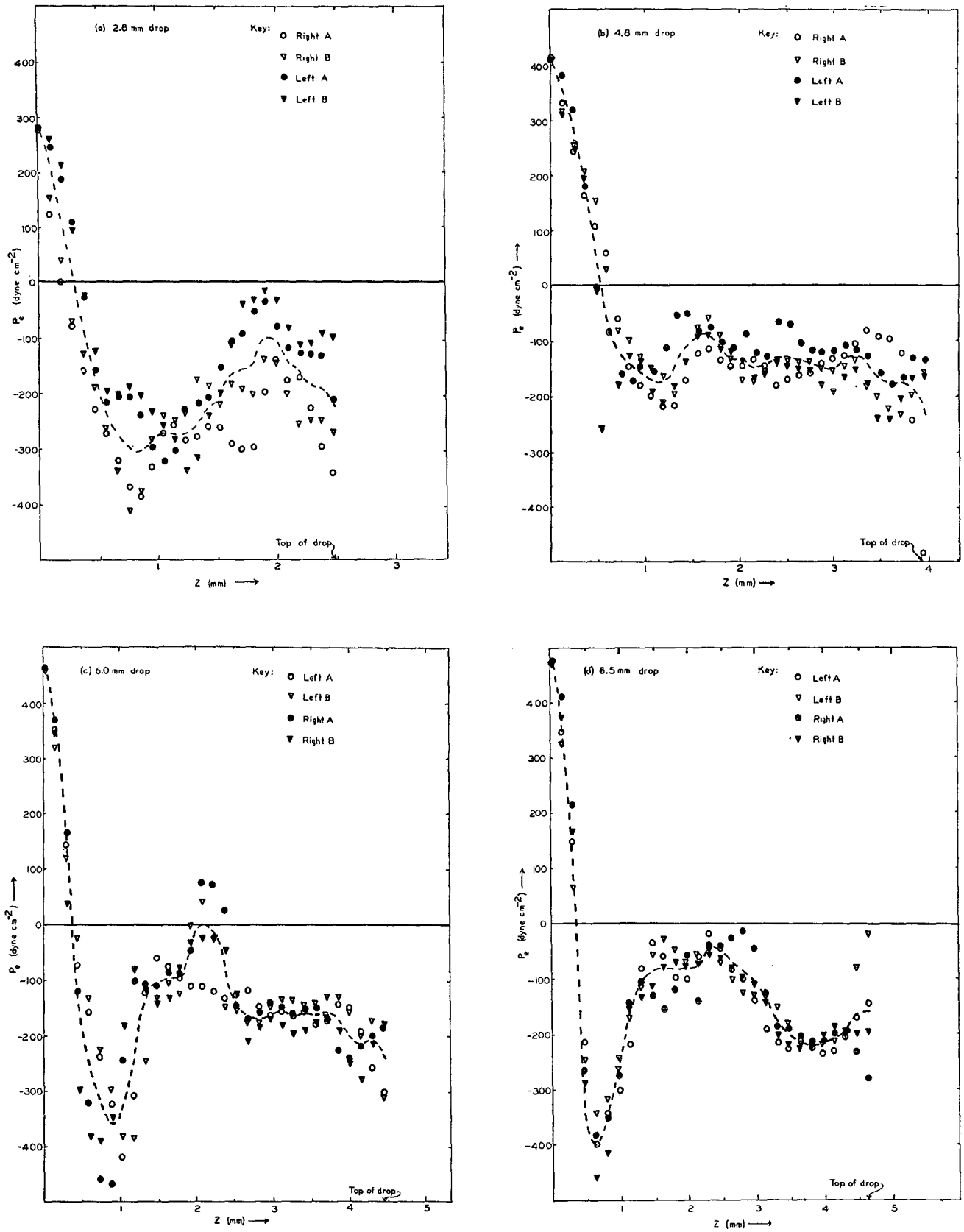

FIG. 4. Computed aerodynamic pressure profiles for four drops of Fig. 1. For each drop, results of four independent analyses are plotted. Abscissa is height above lower stagnation point of each drop. Dashed curves are drawn through means of four computed pressures at each level z.

left) on its upper surface. Examination of all the steps in the calculation for this region on the 2.8-mm drop revealed that this large dispersion was not due to serious errors in construction of normals nor to junction errors, but rather resulted from a peculiar sensitivity of $p_e(z)$ to small errors in just this portion of the profile. For this particular level, it happens that the internal pressure $p_i(z)$ is so nearly equal to the local values of $\Delta p_s(z)$ that $p_e(z) \equiv p_i(z) - \Delta p_s(z)$ is unusually sensitive to any small errors in $\Delta p_s(z)$. Thus, at the level where one of the calculated external pressures for the left-hand profile rises to about -12 dyne/cm^2, one of the right-hand profiles exhibits a pressure of -140 dyne/cm^2, yet the corresponding values of Δp_s differ by only about 12 per cent. Scrutiny of the raw data for this part of the 2.8-mm analyses suggests to the writer that the left-hand profiles are more suspect than their right-hand counterparts; one additional analysis of the left-hand profile tends to confirm this, but the original results are presented here as evidence of the level of error inherent in the method. It is of interest to note that, under just such conditions of computational instability as this, there exists very marked *physical stability* of the drop profile, for the drop *shape* in such a region will be insensitive to rather wide variations in the external aerodynamically controlled pressure. It is in the regions of great computational stability (for the method used here) that the drops themselves must exhibit the greatest configurational instability.

The several profiles provide some evidence of the importance of one type of error in normal construction that was, in fact, anticipated before any pressures were actually computed. At both the lowest and highest point on any profile of a drop which is a true surface of revolution, R_1 and R_2 must converge to a single value which is very large. In reproduction of the photographic profiles with the aid of French curves, it was found difficult to obtain synthetic curves which crossed the symmetry axis at exactly 90 deg. Several auxiliary aids designed to assure this were tried, and the prism device was finally employed in such a way as to check normality; but as soon as analysis was begun, it appeared that there may have been a slight systematic error in curve fitting near the top and the bottom of many of the profiles. This error was such as to yield underestimates of the radius of curvature at the poles of the drop. At the tops of the drops, this effect would have contributed to the rather marked dip toward negative pressures that can be seen in the last few computed points for about half the drops. At the bases of the drops, the method employed prevents this error from producing fluctuations in $p_e(0)$, for the latter was *set* equal to the stagnation-point pressure in every case. However, if such an error occurred at the base of any drop, it will be seen that it would have had the unfortunate effect of displacing, by the constant amount of the error in $\Delta p_s(0)$, all of the remainder of the $p_i(z)$ values and hence also all of the remainder of the $p_e(z)$ values. Actually, inspection of the results does not, in fact, indicate that this occurred, for the scatter in individual values of $p_e(z)$ nowhere appears removable by a simple vertical displacement of one or more full profiles.

As a prominent instance of the discrepant results that can be obtained in the neighborhood of junctions between neighboring curve segments, the odd peak in pressure about halfway up the profile for the 6.0-mm drop (fig. 4, bottom left) is to be noticed. In three of the four curve-fitting processes, a junction fell at this level, and by chance the fitted curves were so chosen as to give a too-flat section here. The result was to give erroneously large values of $R_1(z)$ [though, of course, fairly acceptable values of $R_2(z)$], and hence too-small values of $\Delta p_s(z)$, and, in turn, values of $p_e(z)$ which were more positive than they should have been. This happened to be a level within this drop where the internal pressure was sufficiently close to the corresponding values of Δp_s that the sort of abnormal sensitivity to small errors in Δp_s noted earlier occurred again. The result was that some of the computed external pressures turned out to be positive for this portion of three of the 6.0-mm profiles. Here, as before, the results are displayed as they were first obtained, to illustrate the difficulties that arise in this method of deduction of the external pressure profile around drops.

Examination of the computation data indicates that the level of error in determining $\Delta p_s(z)$ values, as shown by the differences between the eight pairs of analyses in which each pair represented the same half-profile, was considerably larger than that which could be ascribed to the technique for constructing normals. The latter was found to be both accurate and precise to within better than 1 per cent, while the differences in $\Delta p_s(z)$ between members of pairs was of the order of 10 per cent. The writer sees no way other than replication to eliminate these errors of curve reproduction, for the eye does not seem capable of discerning goodness of fit with an accuracy desired in this problem. Perhaps more elaborate optical and photographic techniques might be employed in the original high-speed photography, in order that sharper definition of the profile might be obtained, and curve fitting thereby obviated, but this seems unlikely.

5. Validity of shape hypothesis

To review the logic of the present study, it must be noted that it has not been found possible here to predict the aerodynamic pressure effects on drop shape by proceeding directly from fundamental principles of fluid dynamics; instead, the aerodynamic pressures have been *deduced* from the writer's hypothesis of drop

shape. Therefore it follows that the test of the correctness of the shape hypothesis must involve a comparison between the results shown in fig. 4 and any available and pertinent experimental data.

Experimental evidence for separation.—It is understandable that the literature of experimental aerodynamics does not contain any data on observed pressure patterns around objects of raindrop shape, since this is a quite unusual shape. Furthermore, it would not be easy to set about securing precisely the data desired, because of the following considerations. If a "model" of a large raindrop were to be fabricated with an array of static pressure orifices distributed over its surface, the necessary internal tubing would probably preclude use of a model smaller than 4 or 5 cm in cross section, *i.e.*, the model would have to be six or seven times *larger* than the prototype. To preserve dynamic similarity between model and prototype in the Reynolds sense, the experimental velocity could be only one-sixth or one-seventh of the prototype velocity of fall (about 8 m/sec) if air were used as the model medium; but at such low air speeds, the uncertainties in measurement of the slight static pressure changes involved would pose very serious difficulties.

In view of the lack of precisely the type of observational data needed for comparison with the present results, it becomes a next-best substitute to use data on spheres. Even for spheres, one finds a gap in the experimental results for Reynolds numbers lying between the upper limit of the Stokes-law range and the lower limit of the region of critical Reynolds numbers for transition to a turbulent boundary layer. *Drag* data were found to be abundant for the entire range, but not surface *pressure* data. Thus, it has only been possible to make a comparison with pressure profiles for spheres at Reynolds numbers (denoted below by Re) of the order of 10^5 (Fage, 1937).

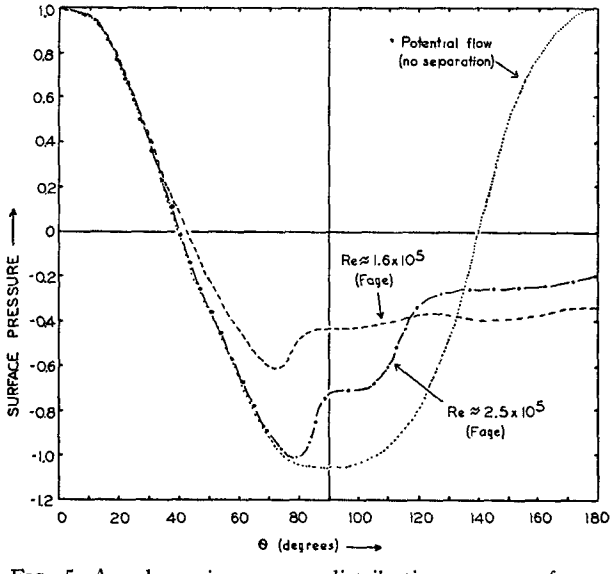

FIG. 5. Aerodynamic pressure distributions over surfaces of spheres for three different flow conditions. Pressure units on ordinate represent excess of actual pressure over free-stream pressure and are plotted non-dimensionally in terms of multiples of stagnation pressure, $\frac{1}{2}v^2$.

Two of Fage's curves for the profile around a sphere (for Re $\approx 2.5 \times 10^5$ and $R \approx 1.6 \times 10^5$) are plotted here in fig. 5. The similarities between these curves and those of fig. 4 are sufficient to provide considerable assurance that the present drop-shape hypothesis is at least fairly close to the truth. The pressures around the downstream hemisphere of Fage's sphere, like those deduced here for the upper surfaces of the large drops, fail to return to positive values (as do the pressures in potential flow, dotted curve of fig. 5) after starting to rise fairly rapidly just ahead of the region of maximum cross section. Now, it is well known that this feature, in curves such as those of fig. 5, is due to the occurrence of "separation" in the boundary layer. At Reynolds numbers below those for which the boundary layer becomes turbulent (Re $\approx 4 \times 10^5$) but above the Stokes-law range (Re ≈ 1), the streamlines fail to close in downstream from the sphere; and by this failure to create a downstream stagnation point, the pressures remain low beyond the zone of separation. The fact that the pressures deduced here for large water drops do exhibit this behavior may be regarded, then, as constituting fairly strong evidence in favor of the shape hypothesis used to determine these pressures. In still further support of this conclusion, there exist two experimental observations on actual water drops which will next be shown to be quite consistent with the present deduction of separation in the air flow around large raindrops.

First, Gunn (1949) has reported a curious tendency for drops of one certain size (about 0.5-mm radius) to undergo marked side-slipping as they fall. Gunn has shown very convincingly that this must be due to a resonance phenomenon involving the natural frequency of mechanical oscillation of the drops and the frequency with which eddies are shed from the upper surface of the falling drop. Gunn invoked Moeller's (1938) extensive results on eddy frequencies for spheres to show that a sphere of 0.5-mm radius sheds eddies at a frequency of about 300 cycle/sec, almost exactly the natural frequency of ellipsoidal vibration of a water sphere of that size. Gunn's detection of this eddying phenomenon really constitutes experimental evidence for separation, since eddies can only be shed from a "deadwater" region bounded by a separating stream surface extending downstream from an object. Furthermore, Gunn's observations concerned a drop size much smaller than the ones here analyzed; so at the higher Reynolds number at which the 2.8- to 6.5-mm drops fell, separation should almost certainly be expected (and this the more so because of the sharper curvature on the upper surface of the larger and more flattened drops).

Second, Blanchard (1950) reported that, when one drop of appropriate size is inserted into the air stream above another drop which is aerodynamically suspended in a vertical air stream, the upper descends upon the lower along a peculiar spiral path. Winny (1932) has, by means of photographs of the flow behind spheres at which separation was occurring, illustrated what appeared to be a spiral eddy pattern in the interval Re $\approx 2 \times 10^3$ to 8×10^3, so Blanchard's observations may be taken as further evidence for separation in the flow around water drops. A very complete discussion of the wake phenomena behind *solid* spheres has been given by Moeller (1938), who concluded that separation first appears at about Re = 150 and that periodic eddy detachment begins at about Re = 450 for solid spheres. For a somewhat deformed drop, these phenomena would be expected to appear at even lower Reynolds numbers.

In all, there seems to be very good reason for believing that separation occurs in the air flow around all raindrops with diameters greater than about 0.5 to 1.0 mm. The fact that the present shape hypothesis has led to the deduction of a pressure profile of a type entirely different from that obtained with potential flow, but quite similar to that characteristic of viscous flow at high Reynolds number, provides one reason for accepting the shape hypothesis adopted here. Quantitative reasons for accepting the hypothesis will now be discussed.

Comparison of drag and weight of drops.—A quantitative test can be based upon the fact that the weight of a drop falling at terminal velocity must be exactly counterbalanced by the vertical components of all the pressure forces and shear-stress forces acting over its surface. The weight of each drop studied here is known, the vertical components of the previously computed aerodynamic forces can be determined, their surface integral can be calculated numerically, and finally the contribution of the integrated shear stresses can be found approximately. With these, an approximate quantitative check can be carrried out.

To compute the resultant, in the vertical direction, of all the aerodynamic forces on the drop, the surface zones already employed in the earlier calculations (see section 3, above) were used. A representative computation is presented in table 2 for the pressure values found in one of the four analyses of the drop of 6.0-mm equivalent diameter (fig. 4, bottom left). For each of the 30 zones into which the drop was divided, table 2 shows the computed external pressure, the vertically projected area of the surface of the zone, and the upward force on the zone due to the external pressure.

A number of interesting features of the distribution of pressure drag over the surface of a raindrop is revealed by computations such as that displayed in table 2. The total upward pressure drag of 103.9 dynes for this particular calculation is the difference between a positive (upward) contribution of 129.8 dynes from the region just around the lower stagnation point and the region above the level of maximum cross section (between zones 10 and 11) and a negative contribution of −25.9 dynes made by the fourth to ninth zones. In the latter portion of the drop, the aerodynamic pressures have already gone negative while the outward normals to the surface zones still possess downward components. Of the 129.8 dynes positive upward drag, 70.1 dynes are the contribution of the region just around the lower stagnation point, while 59.7 dynes are contributed by the *deficient* pressures established over the upper surface of the drop by the effects of boundary-layer separation. This general pattern appeared in each of the sixteen drag computations carried out here and is only to be expected as soon as separation is recognized to exist.

In addition to this upward force due to the vertical components of the pressure forces acting over the drop surface, there is a force due to shear stresses acting at the base of the boundary layer. It has not been possible to compute this force with any degree of accu-

TABLE 2. Computation of pressure drag from Left-A profile for 6.0-mm drop. Surface zones are numbered in increasing order from lower stagnation point to upper pole of drop. Each zone is 0.15 mm in vertical thickness for this drop, but vertically projected area of surface of each zone varies as shown in column 2. Zonal area is regarded as negative here if its outward normal has an upward component. Product of corresponding entries in columns 1 and 2 is zonal contribution to pressure drag and appears in column 3.

Zone no.	External pressure (dyne/cm²)	Projected area of zone (cm²)	Upward force on zone (dyne)
1	460	6.0×10^{-2}	27.4
2	349	9.3	32.6
3	143	7.1	10.1
4	− 74	5.3	−3.9
5	−159	2.3	−3.7
6	−239	2.6	−6.2
7	−326	1.6	−5.2
8	−421	1.3	−5.0
9	−311	0.6	−1.9
10	−124	0.0	0.0
11	− 61	0.0	0.0
12	− 76	−0.4	0.3
13	− 97	−0.2	0.2
14	−112	−0.7	0.8
15	−111	−0.9	1.0
16	−120	−0.9	1.1
17	−135	−1.3	1.6
18	−128	−1.1	1.4
19	−119	−1.5	1.8
20	−148	−1.7	2.5
21	−163	−1.9	3.1
22	−157	−2.1	3.3
23	−164	−2.2	3.6
24	−157	−2.9	4.5
25	−179	−2.8	5.0
26	−172	−2.8	4.8
27	−144	−3.0	4.3
28	−150	−3.0	4.5
29	−199	−3.4	6.8
30	−284	−3.2	9.1
	Total upward pressure drag		103.9 dynes

racy, but a rough estimate can be obtained. Consider once more the drop of 6.0-mm equivalent diameter. Replace the actual drop by a sphere of 0.3-cm radius, and introduce spherical coordinates (r, θ, ϕ), where θ is the colatitude measured from the lower stagnation point, and ϕ is the azimuthal angle. The shear stress will necessarily be axially symmetric here, and will vary with θ; so, calling this stress T_θ, the tangential frictional force in the direction of the air flow acting on an element of surface area is $T_\theta r^2 \sin\theta \, d\theta \, d\phi$, and the vertical component of this is obtained by multiplication by $\sin\theta$. This cannot be integrated until T_θ is given as a function of θ. It is known from wind-tunnel studies on spheres (Goldstein, 1938) that T_θ is zero at the stagnation point and increases with θ up to a point a short distance ahead of the separation point (in a flow characterized by this phenomenon). Since separation normally occurs near $\theta = 80$ deg for spheres, one will overestimate the total shear stress effect if he takes as a crude approximation, $T_\theta = k \sin\theta$, where k is a dimensional constant to be determined. Such a representation for T_θ permits one to integrate the expression for the shear stress. The result, for the lower hemisphere of a sphere of radius r, is $(4/3)(\pi k r^2)$. To evaluate k approximately, the boundary layer theory of Tomotika (1935) may be used. For a drop of 0.3-cm radius falling at about 8 m/sec, the boundary layer thickness is about 0.5 mm at $\theta = 90$ deg. Assuming that the shear stress at this point is given simply by the absolute viscosity multiplied by the average velocity gradient through a boundary of such thickness, one finds that k must equal about 6 dyne/cm^2, an estimate that the writer feels to be in error by no more than a factor of two or three. Putting this estimate of k into the integral of the upward components of the shear stresses, one finds that these stresses total only about 2 dynes over the lower hemisphere of the drop. Since the vertical resultant of the pressure forces has been shown above (table 2) to be about 100 dynes, this estimate of the total vertical shear-stress component could be off by a factor of two without affecting the conclusion that shear stresses contribute only slightly to the total drag on large drops, a conclusion which might have been anticipated from aerodynamic experience, since form drag due to separation effects usually assumes much more importance than skin-friction drag for Reynolds numbers in the raindrop range.

Addition of this crude estimate of 2 dynes due to frictional drag to the previous estimate (for profile Left-A) of about 104 dynes due to the vertical pressure drag gives 106 dynes as the computed total upward force on the drop. The actual weight of the 6.0-mm drop is 110 dynes, so the present shape hypothesis has led, in this one case, to computed drag forces equal to about 96 per cent of the actual drag forces that must have been acting on this drop as it fell at terminal velocity. This discrepancy of −4 per cent is smaller than most of the other fifteen drag-weight discrepancies. A complete summary of the sixteen computations is shown in table 3. Because the surface frictional drag is smaller than the inherent error of the analytical method and difficult to estimate with accuracy, no allowance has been made in any of the drag-weight comparisons for the contribution of friction.

Table 3 shows that the discrepancies between pressure drags computed on the present drop-shape hypothesis and the known weights of the drops average, in absolute value, about 10 per cent. This level of error is very close to that found for the discrepancy in principal radii of curvature as measured from two independently reproduced profile curves, suggesting that most of the mean error for all sixteen analyses may be accounted for in terms of curve-reproduction errors. As further evidence of this, the percentage difference between pressure drags computed for the two members (A and B) of each pair of profiles traced from a given half-drop averaged 7 per cent for the set of eight pairs. It has already been pointed out that the optical technique used to determine normals introduces an error of slightly less than 1 per cent, so curve tracing must account for most of this 7-percent mean difference between members of pairs, and hence must also explain most of the mean error of about 10 per cent in drag forces. The mean coefficient of variation within sets of four pressure analyses is found to be about 8 per cent, so once again curve-tracing errors suffice to explain most of this variability.

The algebraic mean error of all 16 analyses is about −9 per cent, when the drags are compared with the known weights. If one could make accurate estimates of frictional drags and add these to the computed

TABLE 3. Summary of pressure-drag computations and comparisons with known weights of drops. Tabulated coefficients of variation indicate relative scatter of each set of four computed pressure drags about mean of that set. Tabulated errors show percentage error of mean of each set of four computed drags (frictional contribution neglected) compared to known weight of drop.

Equivalent drop diameter (mm)	Pressure drag (dynes)					Coefficient of variation	Weight of drop (dynes)	Error
	Rt-A	Rt-B	Lft-A	Lft-B	Mean			
2.8	9.3	8.8	9.7	10.0	9.5	5%	11.2	−15%
4.8	57.5	63.8	53.2	55.0	57.4	7	56.3	+ 2
6.0	93.9	110.0	103.9	97.5	101.4	6	111.0	− 9
6.5	135.0	121.5	126.1	108.6	122.8	8	141.1	−13

form drags, this mean algebraic error would be reduced; but the crude estimate carried out above shows that frictional drag is only about 2 per cent of the form drag for the 6.0-mm drop, so residual discrepancy would almost surely remain. However, it is felt that the unexplained discrepancy between drag and weight is small enough here to provide fairly strong evidence that the present shape hypothesis is substantially correct.

6. Implications of separation

It should be emphasized that the present calculations of $p_e(z)$ have interest not only in that they provide a check on the present theory of drop shape, but also in that they focus attention on the phenomenon of separation itself. Gunn's (1949) observations imply that this phenomenon is already well established in flow about raindrops of average size (1-mm diameter) falling at Reynolds numbers of less than 300, which finding is in good agreement with Moeller's work on solid spheres. Hence, separation appears to be a phenomenon to be reckoned with in any theory of microphysical processes involving raindrops. The kinematics of ion deposition on falling raindrops, for example, must be affected to some slight extent by the failure for simple potential flow to occur on the upper surfaces of drops. Analyses of heat and water-vapor transfer to or from water drops must take separation into account. That this is so can perhaps be best seen by considering the work of Kinzer and Gunn (1951). Briefly, the time duration of contact between a packet of ambient air and the drop surface is roughly halved by separation at the boundary layer. Also, as Blanchard has found experimentally, the dynamics of a "fall-on" collision between two drops must be sensibly affected by the existence of a pulsatory wake set up behind a drop about which the flow is undergoing separation. The chance that a small drop may coalesce with a larger drop that has overtaken it will be reduced by separation to whatever extent coalescence depends on non-instantaneous processes occurring in the region of contact of the two drops, for separation cuts down the time available for any such rate processes to go to completion. Finally, the size dependence of the terminal velocity of raindrops must be largely due to the well established effect of separation on form drag. For Reynolds numbers in the approximate interval 10 to 10^5, the drag coefficient of a sphere is nearly constant, because in this range form drag (due to the presence of a deadwater region) rather than skin-friction drag is of controlling importance, and separation produces a deadwater region whose dimensions remain roughly independent of Reynolds number until the latter reaches the critical transition value (meteorologically unattainable for raindrops, which break up well below the critical Reynolds number). One can see clearly how important separation is in controlling the form drag on large raindrops by examining the entries in the last column of table 2. The separation point falls at about zone 8. The sum of all the upward forces for zones 9 to 30, 57.8 dynes, is over half of the net upward drag force for the entire drop, a situation strikingly different from that found in potential flow. Altogether, the effects due to separation, whose existence in raindrop aerodynamics seems quite clearly indicated, must constitute a significant factor in the physics of rain.

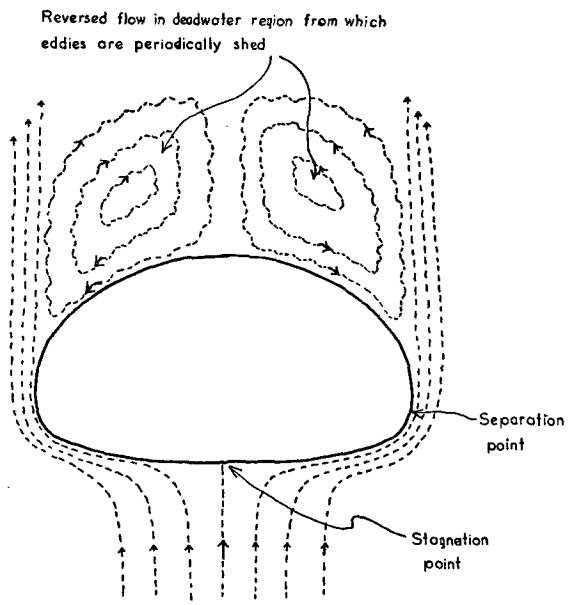

FIG. 6. Suggested mean flow pattern around large raindrop, showing separating boundary layer and turbulent flow in enclosed wake region. That indicated ring vortex in wake cannot have a steady circulation is revealed by existence of quasi-periodic shedding of eddies from upper surface.

The recognition of separation sheds further interesting light on the reason for the probable *non-existence* of appreciable internal circulation inside raindrops. The skin-friction drag at the surface of a liquid drop, about which the flow undergoes separation, is markedly less favorable to the establishment of internal circulation of the spherical vortex type than is the skin-friction drag in the non-separating case. Starting from a zero value at the lower stagnation point, the downstream drag of air on water must reach its maximum value somewhat ahead of the separation point and then must fall once more to zero at the separation point, where, by definition, there exists a zero radial velocity shear right at the drop surface (see Goldstein, 1938, and the suggested flow pattern of fig. 6). Then, downstream from the separation point, there will tend to exist an unsteady ring vortex of reversed circulation concentric with the symmetry axis of the drop. The presence of such a circulation over the upper portion of the drop surface will serve to cut down any incipient internal vortical circulations that do tend to become

established by the drag forces acting over the lower surface of the drop. Hence, once one has recognized that separation is characteristic of the flow around raindrops, he has available a very strong basis for predicting that nothing like a spherical vortex of the Bond (1927) type will occur within large drops, for there simply does not exist a sustained downstream traction of surface air on surface water over the entire surface of the drop. In the analysis of internal circulations carried out above, a surface circulation speed of about 20 cm/sec was predicted for a 5-mm diameter drop. That this result is substantially too large to agree with the observations of Blanchard and of Kinzer is now understandable in retrospect, for in that analysis it was tacitly assumed that the surface air-flow is favorable to generation of a vortical circulation everywhere over the surface of a drop. In reality, the opposing influences of frictional drag at lower and upper surfaces of a drop must be expected to prevent any such strong circulation from developing.

Finally, it is to be noted that separation appears to be responsible for the peculiar asymmetry of a large raindrop with respect to a horizontal plane through its center. It can be shown to be true that, *if* only surface-tension and hydrostatic-pressure effects controlled drop shape, these would produce drops with rounded bottoms and rather flattened tops. However, because a stagnation point inevitably occurs at the *lower* pole, while one cannot develop at the *upper* pole because of separation of the boundary layer, it follows that the lower aerodynamic pressures over the upper surface demand an appreciable larger Δp_s there than on the underside, *i.e.*, the curvature of the upper surface must be greater in order to satisfy the requirement of internal hydrostatic equilibrium in the face of the considerable aerodynamic pressure difference on upper and lower surfaces. Hence, the drop becomes rounded on the top but flattened on the bottom, as revealed by photographs.

7. Summary

The factors affecting the equilibrium shape of large water drops falling at terminal velocity — surface tension, hydrostatic pressure gradients, external aerodynamic pressures, electrostatic charge, and internal circulations — have been examined quantitatively, and only the first three of these have been found to be significant in controlling drop shape. Adopting the hypothesis that the equilibrium shape of a raindrop falling at terminal velocity is that for which the aerodynamic pressures and the surface-tension pressure increments combine to produce just an internal pressure pattern satisfying the hydrostatic equation, the writer found it possible, by analyzing drop photographs, to deduce the aerodynamic pressure profiles along meridians of the drops. These profiles revealed clear evidence of separation of the laminar boundary layer in the air flow around the drops. Since separation effects could also be shown to exist in certain experimental observations, it has been concluded that the working hypothesis for drop shape has been successful in explaining the long-recognized deformation of large raindrops. Furthermore, the drag forces computed from the deduced aerodynamic pressures are in quite good, though not perfect, agreement with the weights of the several drops. A number of implications of separation have been pointed out qualitatively, and it was noted that the distribution of skin-friction drag over the surface of a raindrop at which separation occurs is decidedly unfavorable to the generation of strong internal vortical circulation.

8. Suggestions for future research

Since the present study is regarded by the writer as only a first step towards the more significant objective of understanding the coalescence and breakup of large raindrops, he wishes to take the opportunity to urge extension of the sort of laboratory studies so well begun by Blanchard (1950). The wealth of intriguing questions raised by Blanchard's work, and the light that could potentially be shed on the dynamics of a drop breakup by further studies of this sort, make a continuation of the research most desirable. In this connection, attention is called to a brief critical discussion of Blanchard's work by McDonald (1951), where a number of suggestions for improving this type of study have been offered.

It would be desirable to have rather more conclusive experimental data on the intensities of internal circulation in water drops of various sizes. For drops just below the size for which separation first appears (probably around 0.5-mm diameter), it may be possible that circulation is actually better developed than for larger drops on whose upper surface a reversed flow develops.

Acknowledgment.—Most of the computational work of the present study was done by Mr. Ferdinand Baer of the Department of Meteorology, University of Chicago.

REFERENCES

Adam, N. K., 1949: *The physics and chemistry of surfaces.* London, Oxford Press, 436 pp.

Blanchard, D. C., 1949: *Experiments with water drops and the interaction between them at terminal velocity in air.* Schenectady, Gen. Electric Res. Lab. (Proj. Cirrus, Occas. Rep. No. 17), 29 pp.

——, 1950: The behavior of water drops at terminal velocity in air. *Trans. Amer. geophys. Union*, **31**, 836–842.

Bond, W. N., 1927: Bubbles and drops and Stokes law. *Phil. Mag.*, Ser. 7, **4**, 889–898.

Chalmers, J. A., 1949: *Atmospheric electricity*. London, Oxford Press, 175 pp.

Edgerton, H. E., and J. R. Killian, 1939: *Flash! Seeing the unseen by ultra-high speed photography*. Boston: Hale, Cushman and Flint, 203 pp.

Fage, A., 1937: Experiments on a sphere at critical Reynolds numbers. *Aero. Res. Comm., Rep. and Mem.*, No. 1766, 20 pp.

Flower, W. D., 1928: The terminal velocity of drops. *Proc. phys. Soc. London*, **40**, 167–176.

Garner, F. H., 1950: Diffusion mechanism in the mixing of fluids. *Trans. Inst. chem. Engr.*, **28**, 88–96.

Goldstein, S., 1938: *Modern developments in fluid dynamics*. London, Oxford Press, 702 pp.

Gunn, R., 1947: The electrical charge on precipitation at various altitudes and its relation to thunderstorms. *Phys. Rev.*, **71**, 181–186.

——, 1949: Mechanical resonance in freely falling raindrops. *J. geophys. Res.*, **54**, 383–385.

——, 1950: The free electrical charge on precipitation inside an active thunderstorm. *J. geophys. Res.*, **55**, 171–178.

——, and G. D. Kinzer, 1949: The terminal velocity of fall for water droplets in stagnant air. *J. Meteor.*, **6**, 243–248.

Jeans, J. H., 1941: *The mathematical theory of electricity and magnetism*. Cambridge, Cambridge Univ. Press, 652 pp.

Kinzer, G. D., and R. Gunn, 1951: The evaporation and thermal relaxation-time of freely falling water drops. *J. Meteor.*, **8**, 71–83.

Kluesener, O., 1933: Zum Einspritzvorgang in der kompressorlosen Dieselmaschine. *Z. Verein Deut. Ingr.*, **77**, 171–172.

Laws, J. O., 1941: Measurement of the fall-velocities of water drops and rain drops. *Trans. Amer. geophys. Union*, **22**, 709–721.

Lenard, P., 1904: Über Regen. *Meteor. Z.*, **21**, 248–262.

McDonald, J. E., 1951: Discussion of "The behavior of water drops at terminal velocity in air" by D. C. Blanchard. *Trans. Amer. geophys. Union*, **32**, 775–776.

Macky, W. A., 1931: Some investigations on the deformation and breaking of water drops in strong electric fields. *Proc. roy. Soc. London*, **133**, 565–587.

Magono, C., 1954: On the shape of water drops falling in stagnant air. *J. Meteor.*, **11**, 77–79.

Milne-Thomson, L. M., 1949: *Theoretical hydrodynamics*. New York, Macmillan Co., 600 pp.

Moeller, W., 1938: Experimentelle Untersuchungen zur Hydrodynamik der Kugel. *Phys. Z.*, **39**, 56–80.

Richardson, E. G., 1950: *Dynamics of real fluids*. London, Edw. Arnold, 144 pp.

Spells, K. E., 1952: A study of circulation patterns within liquid drops moving through a liquid. *Proc. phys. Soc. London*, B, **65**, 541–546.

Spilhaus, A. F., 1948: Raindrop size, shape, and falling speed. *J. Meteor.*, **5**, 108–110.

Tomotika, S., 1935: The laminar boundary layer on the surface of a sphere in a uniform stream. *Aero. Res. Comm., Rep. and Mem.*, No. 1678, 14 pp.

Winny, H. F., 1932: Vortex system behind a sphere moving through a viscous fluid. *Aero. Res. Comm., Rep. and Mem.*, No. 1531, 14 pp.